0026-895X/95/030443-08$3.00/0

MOLECULAR PHARMACOLOGY, 48:443–450 (1995).

Comparison of the Pharmacology and Signal Transduction of the Human Cannabinoid CB_1 and CB_2 Receptors

CHRISTIAN C. FELDER, KELLY E. JOYCE, EILEEN M. BRILEY, JALEH MANSOURI, KEN MACKIE, OLIVIER BLOND, YVONNE LAI, ALICE L. MA, and RICHARD L. MITCHELL

Laboratory of Cell Biology, National Institute of Mental Health, Bethesda, Maryland 20892 (C.C.F., K.E.J., E.M.B.), Department of Physiology and Anesthesiology, University of Washington, Seattle, Washington 98195 (K.M., O.B.), Panlabs Inc., Seattle, Washington 98195 (Y.L., R.L.M.), and Howard Hughes Medical Institute-National Institutes of Health Research Scholars Program, Bethesda, Maryland 20892 (J.M.)

Received April 1, 1995; Accepted June 20, 1995

SUMMARY

The recently cloned CB_2 cannabinoid receptor subtype was stably transfected into AtT-20 and Chinese hamster ovary cells to compare the binding and signal transduction properties of this receptor with those of the CB_1 receptor subtype. The binding of [^{3}H]CP 55,940 to both CB_1 and CB_2 was of similar high affinity (2.6 and 3.7 nM, respectively) and saturable. In competitive binding experiments, (−)-Δ9-tetrahydrocannabinol and CP 55,940 were equipotent at the CB_1 and CB_2 receptors, but WIN 55212–2 and cannabinol bound with higher affinity to the CB_2 than the CB_1 receptor. HU 210 had a higher affinity for the CB_1 receptor. Anandamide, a recently identified endogenous cannabinoid agonist, was essentially equipotent at both receptor subtypes. The structurally related fatty acid ethanolamides dihomo-γ-linolenylethanolamide and mead ethanolamide also bound with relatively equal affinity to both receptors, but adrenylethanolamide had a higher affinity for the CB_1 receptor. The rank order of potency and efficacy for binding of the selected agonists to the CB_1 and CB_2 receptors was mimicked in functional inhibition of cAMP accumulation experiments for all compounds tested. Both CB_1 and CB_2 receptors couple to the inhibition of cAMP accumulation that was pertussis toxin sensitive. SR141716A, a CB_1 receptor antagonist, was a poor antagonist at the CB_2 receptor in both binding and functional inhibition of cAMP accumulation experiments. When expressed in AtT-20 cells, the CB_1 receptor mediated an inhibition of Q-type calcium channels and an activation of inward rectifying potassium channels. In contrast, the CB_2 receptor did not modulate the activity of either channel under identical assay conditions. Similar to results obtained for CB_1 receptor, the CB_2 receptor did not couple to the activation of phospholipases A_2, C, or D or to the mobilization of intracellular Ca^{2+}. Except for its inability to couple to the modulation of Q-type calcium channels or inwardly rectifying potassium channels, the CB_1 and CB_2 receptors display similar pharmacological and biochemical properties.

The cannabinoids, which include (−)-Δ9-THC, the active principle in marijuana, are a large and diverse group of lipophilic compounds that mediate both psychoactive and systemic physiological effects such as analgesia, anticonvulsion, immunosuppression, and the alleviation of both intraocular pressure and emesis (1). The cannabinoids exert their effects by binding selectively to G protein-coupled cannabinoid receptors located in the plasma membrane (2). Two subtypes of cannabinoid receptor have been cloned, CB_1 (3) and CB_2 (4). The CB_1 receptor is mainly distributed in the central nervous system, with the highest levels found in the cerebellum, hippocampus, and striatum (5–7) and lesser amounts found in the testis (8). The CB_2 receptor has only recently been cloned, and preliminary studies show its distribution to be predominantly in peripheral tissues, including the marginal zone of the spleen, and in macrophages (4).

Previous pharmacological studies established the presence of cannabinoid agonist binding sites in the central nervous system (9) and their functional coupling to the inhibition of both adenylate cyclase (10) and N-type voltage-dependent calcium channels (11, 12). Cannabinoid agonists can also stimulate arachidonic acid release and inhibit its uptake (13, 14), although cannabinoid receptor involvement was not fully

This project was funded in part by SBIR Phase I Grant No. 1 R43DA09203–01 to Panlabs, Inc., by The Keck Foundation, by a McKnight Research Award, and by National Institutes of Health Grants NS01588, DA08934 and NS08174.

ABBREVIATIONS: (−)-Δ9-THC, (−)-Δ9-tetrahydrocannabinol; arachidonic acid, eicosa-5*Z*,8*Z*,11*Z*,14*Z*,-tetraenoic acid (20:4, n−6); mead acid, eicosa-5*Z*,8*Z*,11*Z*-trienoic acid (20:3, n−9); dihomo-γ-linolenic acid, eicosa-8*Z*, 11*Z*, 14*Z*-trienoic acid (20:3, n−6); adrenic acid, eicosa-7*Z*, 10*Z*, 13*Z*, 16*Z*-tetraenoic acid (22:4, n−6); anandamide, arachidonylethanolamide; adrenylethanolamide, docosatetraenylethanolamide; mead ethanolamide, eicosatrienylethanolamide; CHO, Chinese hamster ovary; L, Ltk$^-$; PCR, polymerase chain reaction; PMSF, phenylmethylsulfonyl fluoride; TLC, thin layer chromatography; HEPES, 4-(2-hydroxyethyl)-1-piperazineethanesulfonic acid; EGTA, ethylene glycol bis(β-aminoethyl ether)-*N*,*N*,*N*′,*N*′-tetraacetic acid.

established. These previous signal transduction studies used brain-derived homogenates, synaptosomes, or cell lines as a source of CB_1 receptor where the presence of other competing receptors could not be ruled out.

More recently, transfection and expression of CB_1 receptor cDNA into mammalian cells has provided a model system in which to investigate subtype-specific binding and signal transduction (15). The expressed CB_1 receptor was shown to bind cannabinoid agonists and couple to the inhibition of adenylate cyclase with the same rank order of potency shown for cannabinoid agonists in brain-derived cells and membranes. Cannabinoid agonists stimulated the release of arachidonic acid, inhibition of arachidonic acid uptake, and intracellular calcium release in both CB_1-expressing cells and untransfected control cells over a similar concentration range, indicating that these processes were cannabinoid receptor independent. With the same model system, the novel cannabimimetic eicosanoid anandamide (16) was identified as an endogenous cannabinoid agonist at the CB_1 receptor in both binding and functional experiments (17). Relatively little is known about the pharmacology or signal transduction of the recently discovered CB_2 receptor.

In the present study, the CB_2 receptor was transfected and stably expressed in CHO and AtT-20 cells to compare receptor pharmacology and signal transduction with those of the CB_1 receptor. Cannabinoid agonists widely used in cannabinoid research were included in the study, as were endogenous fatty acid ethanolamides known to be bioactive at the CB_1 receptor (17). The signal transduction of the CB_2 receptor was investigated to determine whether receptor activation led to similar responses as those observed for the CB_1 receptor, such as coupling to the inhibition of adenylate cyclase or modulation of ion channel function.

Experimental Procedures

Materials. [*side chain*-2,3,4-^{3}H]CP 55,940 and [5,6,8,9,11,12,14,15-^{3}H]arachidonic acid were purchased from New England Nuclear (Boston, MA). [^{3}H]Anandamide was a gift from Dr. David Ahearn (New England Nuclear, Boston, MA). RO-20,1724, a phosphodiesterase inhibitor, was purchased from Biomol (Plymouth Meeting, PA), and Fura-2/AM was obtained from Molecular Probes Inc. (Eugene, OR). Arachidonic acid, adrenic acid, dihomo-γ-linolenic acid, and mead acid, used in the synthesis of fatty acid ethanolamides, were obtained from Biomol. Anandamide, dihomo-γ-linolenylethanolamide, adrenylethanolamide, and mead ethanolamide were synthesized and purified by TLC as previously described (16). CP 55,940 was generously provided by Dr. Larry Melvin (Pfizer Inc., Groton, CT.), WIN 55212–2 by Dr. Susan Ward (Sterling-Winthrop Research Institute, Malvern, PA), HU-210 by Dr. Raphael Mechoulam (Hebrew University, Jerusalem, Israel), and (−)-Δ-9-THC by National Institute of Drug Abuse. All other reagents were purchased from Sigma Chemical Co. (St. Louis, MO). All assays were performed in glass test tubes, which were treated overnight by exposure to dimethyldichlorosilane vapor under vacuum.

Transfection and stable expression of CB_1 and CB_2 receptors in mammalian cell lines. CHO, murine L, and AtT-20 cells were obtained from American Type Culture Collection (Rockville, MD) and maintained as previously described (3, 18). AtT-20 cells, a mouse pituitary cell line, were grown in Dulbecco's modified Eagle's medium supplemented with 10% horse serum, 50 units/ml penicillin, and 50 μg/ml streptomycin in an atmosphere of 5% CO_2. The human CB_1 cannabinoid receptor cDNA was stably expressed in CHO cells as previously described (15), and the resulting clonal cell line was used for functional studies of signal transduction. The human CB_1 cannabinoid receptor was stably expressed in L cells at high levels of expression, as previously described (3), to facilitate the binding studies. With previously published sequence information (4), the following oligonucleotides were designed to prime PCR amplification of CB_2: 5′ GGAATTCAAGCTTGGATCCGCCCA CCCCATGGAG-GAATGCTGG 3′ (sense strand primer) and 5′GGAATTCAAGCT-TCTCGA GTCAGCAATCAGAGAGGTCTAGATC 3′ (antisense strand primer). PCR amplification of CB_2 sequences from human spleen mRNA was conducted for 30 cycles (96° for 45 sec, 55° for 45 sec, and 72° for 2 min) at a primer concentration of 150 nM, yielding a product that was 1.3 kb long. The CB_2 PCR product was purified by electrophoresis and electroelution and then digested with *Bam*HI and *Xho*I and ligated into the polylinker of the mammalian expression vector pcDNA3 (Invitrogen, San Giego, CA). After confirmation of the inserted CB_2 cDNA sequence, the resulting CB_2 expression vector was transfected into the AtT-20 mouse pituitary cell line by calcium phosphate precipitation. Transfected cells were selected in medium containing G418, and the expression level of CB_2 receptor in clonal lines was determined by saturation analysis with the radioligand [^{3}H]WIN 55212–2. One clone, designated AtT-20-CB_2-D5, was selected for additional radioligand binding studies. Signal transduction studies on the CB_2 receptor were conducted with CHO cells transfected with the CB_2 receptor by the same methods used for CB_1 receptor expression in CHO cells (15).

Plasma membrane preparation and radioligand binding assays. Plasma membranes were prepared from murine fibroblast L cells, AtT-20 cells, rat cerebellum, and rat spleen as previously described (15). Competition binding assays were performed with 0.5 nM [^{3}H]CP 55,940 as the labeled ligand. Radioligand binding of cannabinoid agonists was measured with the use of a previously described rapid filtration assay (15). PMSF was included where indicated to inhibit the degradation of anandamide during radioligand binding experiments (19, 20).

Anandamide degradation was analyzed by incubating [^{3}H]anandamide with plasma membranes prepared from rat cerebellum or L-CB_1 cells under identical assay conditions as those used for the binding experiments. At the end of the 1-hr incubation period, the reaction volume was extracted twice with 3 volumes of toluene. The organic layers were combined, dried under a stream of N_2 gas, resuspended in 15 μl of toluene, and spotted on 250-μm silica gel 60 TLC plates (Whatman, Clifton, NJ). The TLC plates were developed in a solvent system containing $CHCl_3$/hexane/methanol (40:20:4, v/v/v) along with authentic standards and radioactive products detected by autoradiography after spraying the silica gel with surface autoradiography enhancer (NEN Products, Boston, MA).

Analysis of second-messenger pathways. Arachidonic acid release, cAMP accumulation, and inositol phosphate release were determined as previously described (15) and used as an index of phospholipase A_2, adenylate cyclase, and phospholipase C activation, respectively. Changes in intracellular free calcium concentration were measured by loading cells with the calcium-sensitive fluorescent dye Fura-2 as previously described (15). Phospholipase D activation was determined in suspended cells by measuring both phosphatidylethanol and phosphatidic acid release with the use of a modified previously published method (21). Briefly, cells prelabeled for 18 hr with [^{14}C]palmitic acid were washed twice with assay buffer (Eagle's No. 2 media). Cells were incubated with or without anandamide for 15 min in the presence of 1% ethanol and stopped by rapid centrifugation at 4°. Phosphatidylethanol was extracted with methanol/chloroform/H_2O (1:2:1) and analyzed by TLC on silica gel 60A TLC plates developed in chloroform/pyridine/formic acid (50:30:7). Lipids that corresponded to authentic standards were detected and quantified by phosphoimaging. The IC_{50} values for the inhibition of forskolin-stimulated cAMP accumulation were calculated by nonlinear regression analysis of the primary data using the computer software Graph Pad (San Diego, CA).

Electrophysiological recordings. Currents were recorded using the whole-cell voltage-clamp technique (22) with pipettes that had been pulled from microhematocrit glass (VWR Scientific) and then fire polished. For recording, a coverslip containing cells was transferred to a 200-μl chamber that was constantly perfused (1–2 ml/min) with the appropriate external solution. Solution reservoirs were selected with the use of a series of solenoid valves that allowed solution changes in <1 min. Voltage protocols were generated, and data were digitized, recorded, and analyzed using Basic-Fastlab (Indec Systems, Capitola, CA). Junction potentials were uncorrected.

Potassium currents were measured with a pipette solution containing 130 mM KCl, 20 mM HEPES, 10 mM EGTA, 5 mM $MgCl_2$, 3 mM Na_2ATP, 0.6 mM GTP, and 0.08 mM leupeptin, pH 7.25 with KOH. The external solution contained 40 mM KCl, 110 mM NaCl, 1 mM $CaCl_2$, 25 mM HEPES, and 10 mM glucose, pH 7.35 with NaOH. Fatty acid-free bovine serum albumin (3 μM) was added to decrease the adsorption of cannabinoids. The K_{ir} current was defined as the component of the current sensitive to 1 mM Ba^{2+} elicited during the final 150 msec of a 250-msec hyperpolarizing pulse to −100 mV from a holding potential of −45 mV. Currents were sampled at 1 kHz. The magnitude of the K_{ir} current was dependent on cell size; therefore, aggregate current data are presented as current densities normalized to cell capacitance.

Calcium currents were measured with a pipette solution containing 100 mM CsCl, 40 mM HEPES, 10 mM EGTA, 5 mM $MgCl_2$, 3 mM Na_2ATP, 0.2 mM GTP, and 0.08 mM leupeptin, pH 7.30, with CsOH. The external solution contained 160 mM NaCl, 10 mM $BaCl_2$, 4 mM KCl, 1 mM $MgCl_2$, 10 mM HEPES, and 8 mM glucose, pH 7.35, with NaOH. Tetrodotoxin (200 nM) was added to block sodium currents, and fatty acid-free bovine serum albumin was added to decrease the adsorption of cannabinoids. I_{Ca} was measured near the end of a 25-msec depolarization pulse to 0 mV from a holding potential of −90 mV and was defined as that component of the current sensitive to 100 μM $CdCl_2$. Currents were sampled at 4 kHz. To control for possible response variations with passage number and to avoid sources of systematic bias, experimental and control measurements were alternated whenever possible, and concurrent controls were always performed. Data are expressed as the mean ± standard error.

Results

Stable expression of the CB_2 receptor in CHO (CHO-CB_2) and AtT-20 (AtT-20-CB_2) cells. The CB_2 receptor was stably expressed in CHO and AtT-20 cells as described in Experimental procedures. Saturation binding studies were performed with plasma membranes prepared from both CHO-CB_2 and AtT-20-CB_2 cells with [^{3}H]CP 55,940 used as the labeled ligand (Fig. 1). Identical saturation binding experiments were performed with plasma membranes prepared from rat spleen as an endogenous source of CB_2 receptor (Fig. 1). [^{3}H]CP 55,940 bound with relatively similar affinity to CHO-CB_2 and AtT-20-CB_2 plasma membranes and with a higher affinity to rat spleen plasma membranes. The AtT-20-CB_2 cells were used for all subsequent radioligand binding experiments, and the CHO-CB_2 cells were used for functional inhibition of adenylate cyclase.

The inhibition constants (K_i) for the competition of selected cannabinoid agonists with 0.5 nM [^{3}H]CP 55,940 for binding to AtT-20-CB_2 and L-CB_1 cell membranes are listed in Table 1. Functional inhibition of forskolin-stimulated cAMP accumulation was measured in CHO-CB_2 and CHO-CB_1 cells, and the resulting IC_{50} values are given in Table 2. Several commonly used cannabinoid agonists were tested, and the corresponding data are given (Tables 1 and 2, top). Anandamide and fatty acid ethanolamides shown to be agonists at

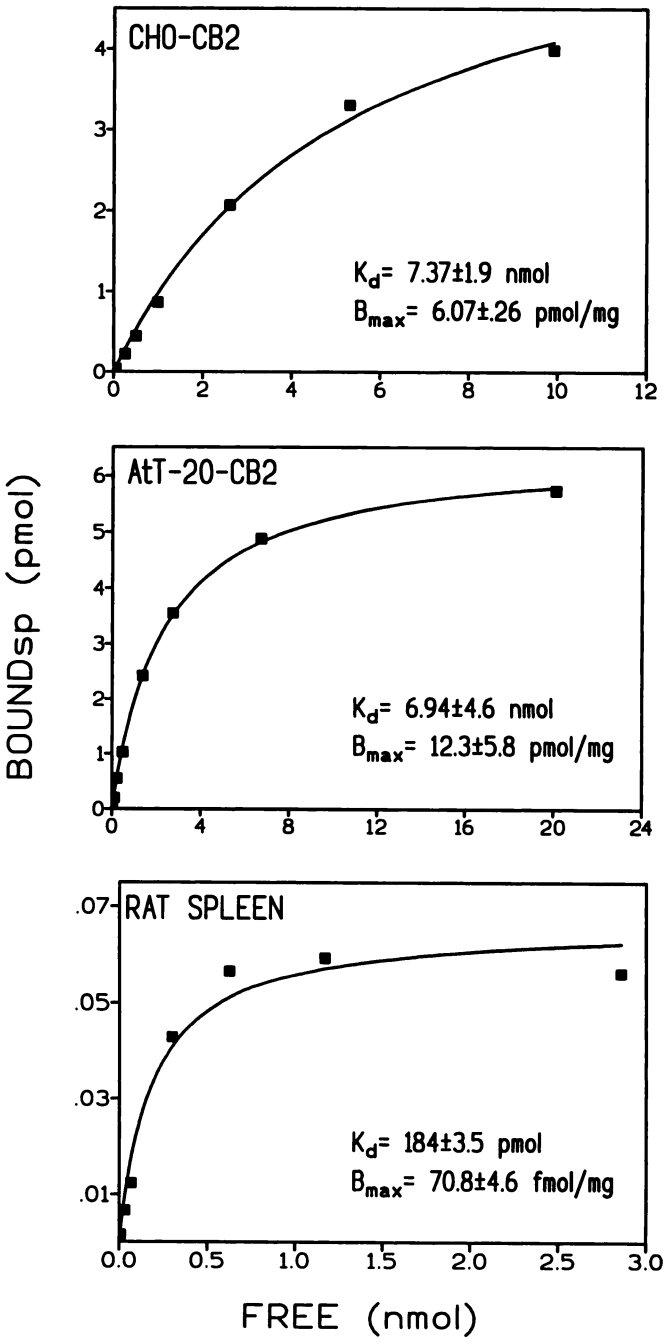

Fig. 1. Specific binding of [^{3}H]CP 55,940 to AtT-20-CB_2, L-CB_1, and rat spleen cell membranes. Plasma membranes were prepared from AtT-20 and CHO cells stably transfected with the CB_2 receptor (AtT-20-CB_2 and CHO-CB_2, respectively) and rat spleen cell membranes, as described in Experimental procedures. Specific binding was defined as the amount of [^{3}H]CP 55,940 bound in the presence of 10 μM HU210 (to saturate specific binding) subtracted from total [^{3}H]CP 55,940 bound at each concentration point. Saturation binding isotherms were analyzed with nonlinear regression analysis, and the derived binding constants are the mean ± standard deviation of at least two experiments, each performed with triplicate determinations. *Curves*, representative experiments.

the CB_1 receptor were also tested for binding and functional inhibition of adenylate cyclase (Tables 1 and 2, bottom). HU-210, a very potent agonist structurally related to (−)-Δ9-THC, was more selective for the CB_1 than the CB_2 receptor, with a CB_1-to-CB_2 dose-response ratio of 8.6. (−)-Δ9-THC

TABLE 1

Inhibition constants (K_i) for the competition of selected cannabinoid agonists with 0.5 nM [^{3}H]CP 55,940 for binding to AtT-20-CB_2 and L-CB_1 cell membranes

	AtT-20-CB_2	L-CB_1	Receptor K_i ratio
Agonist	*nM*	*nM*	
HU-210	0.524 ± 0.045	0.0608 ± 0.0070	CB_2/CB_1:8.6
CP 55,940	2.55 ± 0.19	3.72 ± 0.090	CB_1/CB_2:1.5
WIN 55,212–2	3.30 ± 0.40	62.3 ± 31	CB_1/CB_2:19
(−)-Δ^9-THC	75.3 ± 8.4	53.3 ± 8.3	CB_2/CB_1:1.4
Cannabinol	301 ± 110	1130 ± 190	CB_1/CB_2:3.8
DHGL-ethanolamide	857 ± 100	598 ± 260	CB_2/CB_1:1.4
Mead ethanolamide	1800 ± 520	680 ± 48	CB_2/CB_1:2.6
Anandamide	1940 ± 240	543 ± 83	CB_2/CB_1:3.6
Adrenyl-ethanolamide	9020 ± 470	848 ± 100	CB_2/CB_1:11
Antagonist			
SR 141716A	973 ± 280	11.8 ± 2.0	CB_2/CB_1:82

TABLE 2

IC_{50} values for the functional inhibition of forskolin-stimulated cAMP accumulation in CHO-CB_2 and CHO-CB_1 cells.

	CHO-CB_2	CHO-CB_1
Agonist	*nM*	*nM*
WIN 55,212–2	0.407 ± 0.31	24.0 ± 3.7
HU-210	0.578 ± 0.36	0.197 ± 0.012
CP 55,940	2.89 ± 0.0050	1.83 ± 0.24
(−)-Δ^9-THC	41.8 ± 21	16.5 ± 1.2
Cannabinol	>1 μM	>1 μM
Mead ethanolamide	156 ± 29	432 ± 110
Anandamide	957 ± 58	322 ± 58
DHGL-ethanolamide	1160 ± 230	682 ± 350
Adrenyl-ethanolamide	>1 μM	360 ± 193
Antagonist		
SR 141716A	>1 μM	143 ± 11

bound with essentially equal affinity to the CB_1 and CB_2 receptors, as did the somewhat structurally related agonist CP 55,940 (23). The aminoalkylindole WIN 55212–2 was more selective for the CB_2 than the CB_1 receptor, with a CB_2-to-CB_1 dose-response ratio of 19. Cannabinol, which is weakly cannabimimetic (24), was also more selective for the CB_2, with a CB_2-to-CB_1 dose-response ratio of 3.8. Except for the higher affinity of WIN 55,212–2 and cannabinol for the CB_2 receptor, the cannabinoid agonists displayed identical rank order of potency for the CB_1 and CB_2 receptors. Similar results were observed for the functional inhibition of cAMP accumulation in CHO-CB_2 and CHO-CB_1 cells. WIN 55212–2 was more potent in CHO-CB_2 cells than in CHO-CB_1 cells by a factor of 60. The functional coupling of the CB_1 receptor has been observed to occur through a pertussis toxin-sensitive G protein (10). Pertussis toxin, which blocks the function of the heterotrimeric G_i and G_o proteins through ADP ribosylation, attenuated the ability of WIN 55212–2 to inhibit cAMP accumulation in both CHO-CB_2 and CHO-CB_1 cells (data not shown), indicating that they share a common functional coupling mechanism.

Anandamide has been established as an endogenous agonist at the CB_1 receptor (17). However, it is not clear whether anandamide or other cannabimimetic fatty acid ethanolamides are functional agonists at the CB_2 receptor. Anandamide, dihomo-γ-linolenylethanolamide, and mead ethanolamide displayed relatively similar potencies for binding at the CB_1 and CB_2 receptors (Table 1). Adrenylethanolamide had a higher affinity for the CB_1 than the CB_2 receptor, with a CB_1-to-CB_2 dose-response ratio of 11, although its affinity was relatively weak. Similar results were observed for functional inhibition of adenylate cyclase (Table 2).

A recently described cannabinoid antagonist, SR 141716A (25), was also evaluated for CB_1 and CB_2 receptor binding and ability to block anandamide-mediated inhibition of cAMP accumulation in the transfected cell model. SR 141716A had a much higher affinity for the CB_1 than the CB_2 receptor in binding studies, with a dose-response ratio of 82. The antagonist was not able to completely inhibit forskolin-stimulated cAMP accumulation via CB_2 receptor stimulation but had an IC_{50} value of 143 nM at the CB_1 receptor.

Role of anandamide amidase on anandamide binding to cannabinoid receptors expressed in cell lines. It has been suggested that binding constants for anandamide can only be measured reliably in the presence of inhibitors of degradative amidases present in tissue preparations (20, 26). In the absence of these inhibitors, the K_i value for anandamide has been shown to shift to higher values. However, the effect of PMSF on anandamide binding in cannabinoid receptor-transfected cells has not been investigated. Competition of anandamide for [^{3}H]CP 55,940 binding was marginally sensitive to the amidase inhibitor PMSF in rat spleen (Fig. 2A) and more so in cerebellar (Fig. 2B) plasma membrane preparations but not in those prepared from L-CB_1 (Fig. 2A) or AtT-20-CB_2 (Fig. 2B) cells. Furthermore, no detectable loss of [^{3}H]anandamide occurred when incubated with L-CB_1 plasma membranes under identical conditions used for binding studies (Fig. 2C). However, marked degradation of [^{3}H]anandamide occurred in rat cerebellar membranes.

The CB_2 receptor fails to inhibit I_{Ca} or activate K_{ir} current. In AtT-20-CB_2 cells expressing either 1.2 pmol/mg protein (high) or 189 fmol/mg protein (low) of CB_2 receptors, 100 nM WIN 55,212–2 failed to inhibit the calcium current elicited by a step depolarization to 0 mV from a holding potential of −80 mV (Fig. 3A). Anandamide was similarly ineffective in inhibiting Q-type I_{Ca}. However, in AtT-20-CB_1 cells expressing 800 fmol/mg protein CB_1 receptors, 100 nM WIN 55,212–2 consistently inhibited I_{Ca} (Fig. 3A). In all three cell lines, 10 μM oxotremorine-M, a muscarinic agonist, inhibited the high voltage-activated I_{Ca} (Fig. 3A), suggesting that this signaling pathway was not altered by expression of the CB_2 receptor.

In AtT-20-CB_2 cells expressing either 7.6 pmol/mg protein (high) or 189 fmol/mg protein (low) of CB_2 receptors, 100 nM WIN 55,212–2 failed to activate K_{ir} current (Fig. 3B). How-

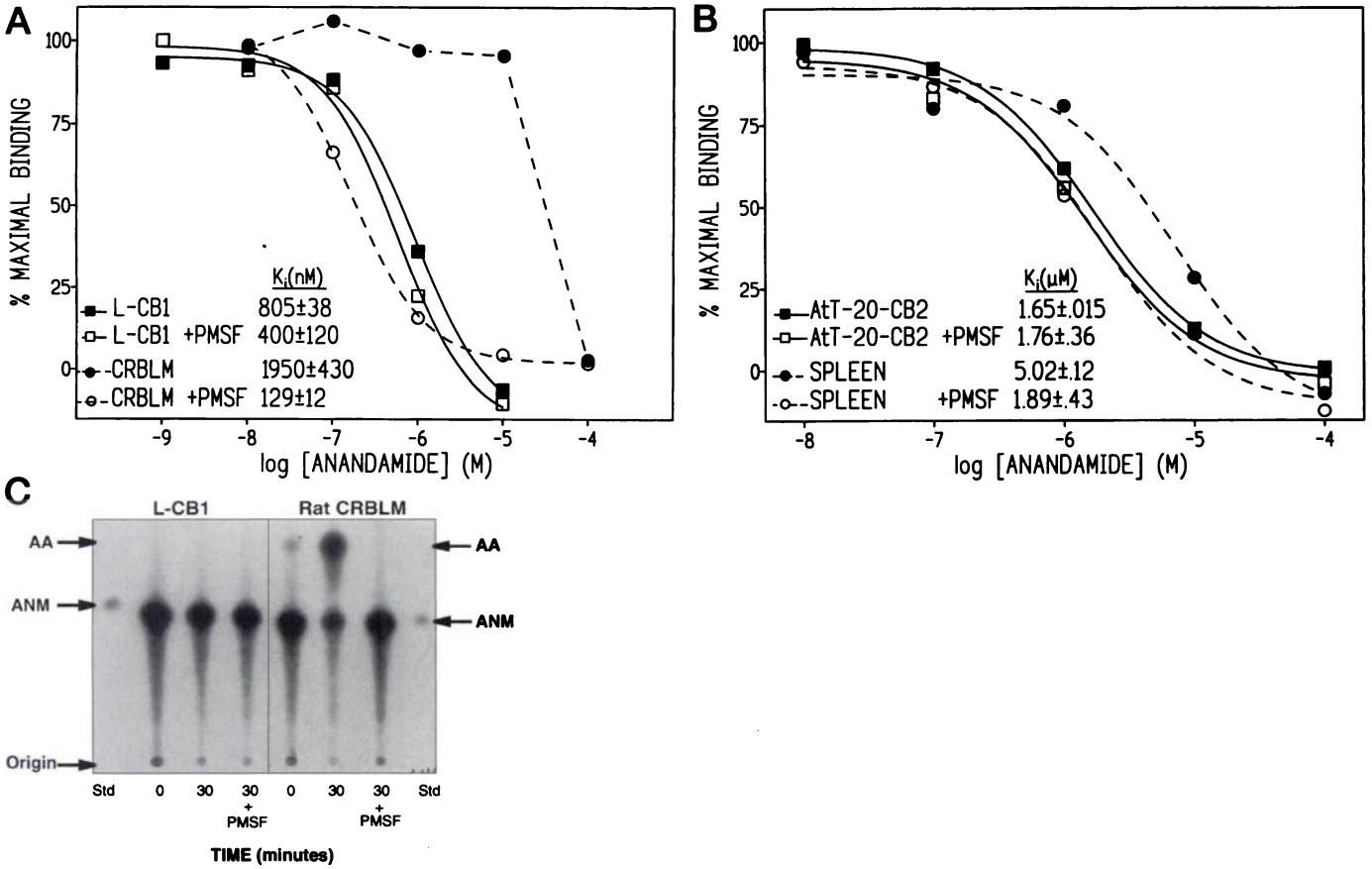

Fig. 2. Absence of anandamide amidase (*ANM*) activity in L and AtT-20 cells. A, L-CB_1 and rat cerebellum (*CRBLM*) plasma membranes. B, AtT-20-CB_2 and rat spleen membranes. Membranes were incubated in the absence or presence of 100 μM PMSF (an inhibitor of anandamide amidase activity). Competition of anandamide for [^{3}H]CP 55,940 (0.5 nM) binding was performed as described in Experimental Procedures, and binding constants were derived by nonlinear regression analysis. Data are the mean ± standard error of at least three experiments, each performed in triplicate. Error bars were removed from the data points for clarity. Standard error did not deviate by >10% of the value of the data points. C, L-CB_1 cells. These cells were incubated with [^{3}H]anandamide under identical conditions used for the binding experiments as described in Experimental Procedures. At the end of the 30-min incubation period, the remaining [^{3}H]anandamide was extracted from the samples and analyzed by TLC. *AA*, Arachidonic acid.

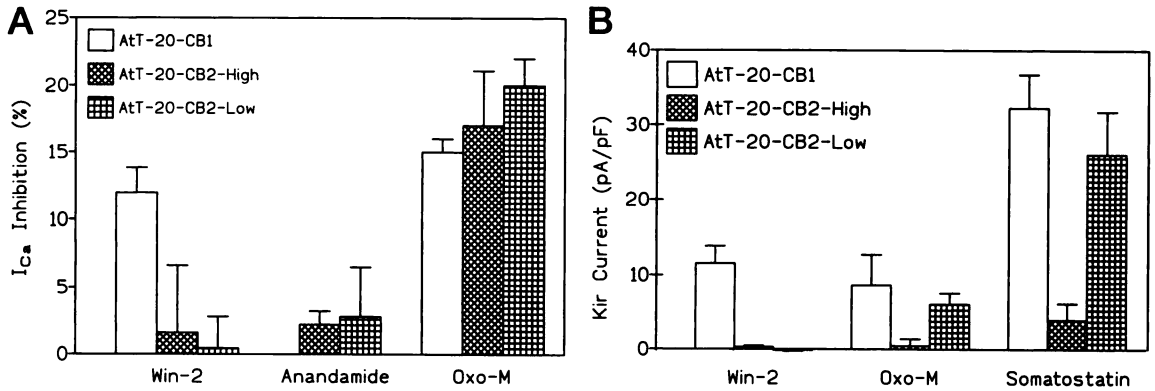

Fig. 3. A, Inhibition of high voltage-activated calcium currents (*ICa*). In AtT-20 cells expressing CB_2 receptors (AtT-CB1), 100 nM WIN 55,212–2 (*Win-2*) and 10 μM oxotremorine-M (*Oxo-M*) consistently inhibited I_{Ca}. However, in cells expressing high (1.2 pmol/mg protein [*AtT-20-CB2-High*]) or low (189 fmol/mg protein [*AtT-20-CB2-Low*]) levels of CB_2 receptor, 100 nM WIN 55,212–2 and 300 nM anandamide were ineffective as inhibitors of I_{Ca}. Oxotremorine-M inhibited I_{Ca} in cells expressing both high and low levels of CB_2 receptor. Data are the mean ± standard error obtained from at least three cells. The effect of anandamide on I_{Ca} in AtT-20-CB_1 cells was not determined. B, Activation of inwardly rectifying potassium current (*Kir*). In AtT-20 cells expressing CB_1 receptor (*AtT-20-CB1*), 100 nM WIN 55,212–2 (*Win-2*), 10 μM oxotremorine-M (*Oxo-M*), and 200 nM somatostatin, all activated a K_{ir} current. WIN 55,212–2 was ineffective in activating a K_{ir} current in cells expressing high (7.6 pmol/mg protein [*AtT-20-CB2-High*]) or low (189 fmol/mg protein [*AtT-20-CB2-Low*]) levels of CB_2 receptor. Oxotremorine-M and somatostatin did not activate K_{ir} current in high expressors of CB_2. However, coupling was preserved in AtT-20 cells expressing low levels of CB_2 receptor. Data are the mean ± standard error obtained from at least three cells.

ever, in AtT-20 cells expressing CB_1 receptor (500 fmol/mg protein), WIN 55,212–2 activated K_{ir} under identical conditions (27). Furthermore, K_{ir} was activated by 10 μM oxotremorine-M and 200 nM somatostatin in cells expressing 189 fmol/mg of CB_2 receptor. In contrast, in AtT-20 cells expressing 7.6 pmol/mg protein of CB_2 receptor, the effects of oxotremorine-M and somatostatin on K_{ir} current activation were abolished.

The CB_2 receptor does not couple to activation of phospholipase A_2, C, or D or mobilization of intracellular calcium in CHO-CB_2 cells. CHO-CB_2 cells were stimulated with anandamide or WIN 55,212–2 over a concentration range of 1 nM to 100 μM. As a control, CHO cells expressing the m5 muscarinic receptor were stimulated under identical assay conditions with the muscarinic receptor agonist carbachol over a concentration range of 1 nM to 10 μM. Neither WIN 55,212–2 nor anandamide had an effect on inositol 1,4,5-trisphosphate generation or phosphatidylethanol formation, second messengers that were measured as an index of phospholipase C and phospholipase D activation, respectively (data not shown). Anandamide stimulated arachidonic acid release in CHO-CB_2 cells and control CHO cells over the same concentration range, suggesting a CB_2 receptor-independent mechanism (Fig. 4). In contrast, WIN 55,212–2 had no effect on arachidonic acid release in CHO-CB_2 or control CHO cells. Under identical assay conditions, carbachol stimulated a dose-dependent increase in arachidonic acid release, inositol 1,4,5-trisphosphate generation, and phosphatidylethanol formation in CHOm5 cells that was blocked with the muscarinic receptor antagonist atropine (data not shown).

Changes in intracellular Ca^{2+} were observed in Fura-2-loaded untransfected CHO control and CHO-CB_2 cells. WIN 55212–2 failed to stimulate any increase in intracellular Ca^{2+} up to 10 μM, the highest concentration tested in both control and CHO-CB_2 cells. However, as previously reported for CHO control and CHO-CB_1 cells (15), HU210 (10 μM) caused an oscillatory increase in intracellular Ca^{2+} that was insensitive to the removal of extracellular Ca^{2+} in both control and CHO-CB_2 cells (data not shown).

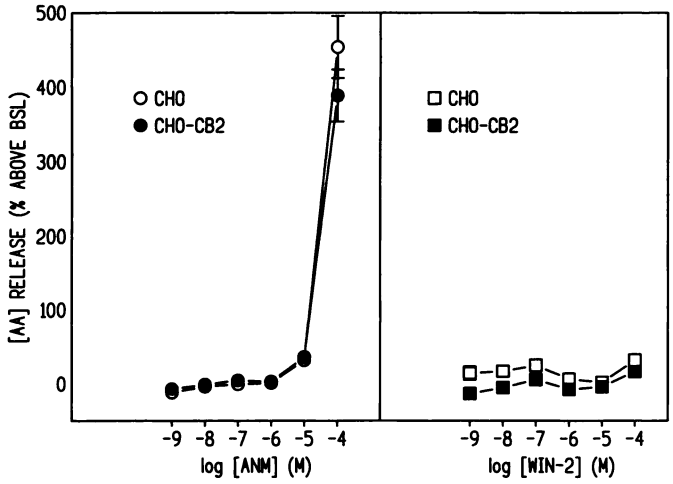

Fig. 4. Release of arachidonic acid is stimulated by anandamide, but not WIN 55212–2, in CHO control and CHO-CB_2 cells. CHO control and CHO-CB_2 cells were labeled overnight with [^{3}H]arachidonic acid (*AA*), and AA release into the media was measured after 15-min stimulation by anandamide (*ANM*) or WIN 55212–2 (*WIN-2*). Data are the mean ± standard error of three experiments, each performed in triplicate.

Discussion

The expression of cDNA for CB_1 and CB_2 cannabinoid receptor subtypes in cell lines provides a convenient system in which to evaluate receptor-specific pharmacology and signal transduction. For the most part, results obtained in expression models compare well with data obtained from tissues expressing endogenous cannabinoid receptors. The binding affinity of CP 55,940, WIN 55,212–2, cannabinol, and anandamide in our cell line (Table 1) were comparable to previously reported values for the CB_2 receptor transiently expressed in COS cells (1.6, 3.7, 250, and 1600 nM, respectively) (4). The binding affinity of (−)-Δ9-THC was higher for our expression cell line than that observed in transiently transfected COS7 cells (4) (75.3 versus 320 nM, respectively), which may simply reflect methodological differences. Little relative difference in affinity for either the CB_1 and CB_2 receptors was observed for CP 55,940 and (−)-Δ9-THC. WIN 55,212–2 and cannabinol had 19- and 3.8-fold higher affinities at the CB_2 than the CB_1 receptor, respectively. WIN 55212–2 is structurally dissimilar to both classic agonists, such as (−)-Δ9-THC, and nonclassic agonists, such as CP 55,940, and therefore may bind to different determinants within the CB_2 receptor structure. The relatively low affinity of cannabinol for the CB_1 receptor may explain its general lack of cannabimetic activity *in vitro*. The data obtained from competition binding curves shown in Table 1 were reflected in the functional studies shown in Table 2, except for SR141716A. The cannabinoid agonist-mediated inhibition of forskolin-stimulated cAMP accumulation in CHO-CB_2 cells was pertussis toxin sensitive, suggesting that the coupling was mediated by G_i or G_o, similar to that observed for the CB_1 receptor. Ectopic expression of G protein-coupled receptors in mammalian cells above physiological levels could lead to an increase in the proportion of receptors in the low affinity uncoupled state, possibly due to an imbalance in the receptor-to-G protein stochiometric ratios. In the present study, clonal cell lines expressing the human CB_1 and CB_2 receptors were selected with similar levels of receptor expression to ensure that the comparison of receptor affinities for selected ligands was valid (see Table 1 and 2 legends for K_d and B_{max} values). Nonlinear regression analysis of saturation binding isotherms for both CB_1 and CB_2 receptor-expressing cell lines fit best to a single binding site, indicating that most of the receptor populations were in a similar affinity state. Although overexpression of receptors in cell lines provides a convenient source of material for pharmacological analysis, more studies will be required to understand the relationship between these pharmacological model systems and the endogenously expressed receptors.

The cannabinoid receptor antagonist SR141716A had a higher affinity for the CB_1 than the CB_2 receptor (Table 1), as previously reported (25). However, SR141716A was not as potent in its ability to inhibit forskolin-stimulated cAMP accumulation (Table 2). This discrepancy was due to a stimulatory effect of SR141716A on forskolin-stimulated cAMP accumulation at concentrations of >500 nM (data not shown). Therefore, the IC_{50} value for SR141716A has both an inhib-

itory and a stimulatory component. The mechanism for the stimulatory effect is not known and is under investigation.

The first endogenous cannabinoid agonist, anandamide, was isolated from porcine brain and consists of a novel eicosanoid structure combining arachidonic acid with ethanolamine in an amide linkage (16). It was subsequently shown that synthetically prepared anandamide, as well as the fatty acid ethanolamides of dihomo-γ-linolenylethanolamide and adrenylethanolamide, was a functional agonist at the CB_1 receptor (17). Dihomo-γ-linolenylethanolamide and adrenylethanolamide have since been identified in mammalian brain (28), but it is not known whether these compounds are synthesized in regions expressing CB_2 receptors. Dihomo-γ-linolenylethanolamide was essentially equipotent at the CB_1 and CB_2 receptors, yet adrenylethanolamide had an 11-fold higher affinity for the CB_1 than for the CB_2 receptor. We have synthesized a novel fatty acid ethanolamide using mead acid and found it to be essentially equipotent to anandamide as an agonist at both receptors. Mead ethanolamide has not been isolated from mammalian tissues, and it is not known whether it occurs naturally. Mead acid, however, is known to accumulate in tissues during periods of fatty acid deprivation (29) and therefore may provide a compensatory mechanism for cannabinoid agonist formation during starvation.

Significant differences have been observed between the affinities of anandamide for the cannabinoid receptors expressed in rat brain membranes and those expressed in cell lines. It was suggested that this difference was due to the inclusion of the protease inhibitor PMSF, as an anandamide amidase inhibitor, in binding experiments (26). In the present study, we were able to reproduce the effect of PMSF on anandamide binding in rat brain membranes; however, we found no effect of this compound on the K_i for anandamide in AtT-20-CB_2 and L-CB_1 membranes. Moreover, degradation of [^{3}H]anandamide did not occur in L cell membranes. It is evident that AtT-20 and L cells lack sufficient levels of anandamide amidase to influence the binding constants derived from our experiments.

The CB_2 receptor did not couple to phospholipase A_2, C, or D or calcium mobilization when expressed in the CHO cells. We have previously reported the stimulation of arachidonic acid release by anandamide and release of Ca^{2+} from intracellular stores in both untransfected CHO control and CHO-CB_1 cells (15). In the present study, we report similar findings for the CB_2-expressing CHO cells. The cannabinoid receptor antagonist SR 141716A failed to inhibit anandamide-stimulated arachidonic acid release at 10 μM in either CHO-CB_1, CHO-CB_2, or CHO control cells (data not shown). Therefore, it is unlikely that the release of arachidonic acid or calcium is mediated by the CB_1 or CB_2 receptor in these cells. In contrast to cannabinoid agonists such as anandamide and HU-210, which stimulate arachidonic acid release, WIN 55212–2 had no effect on either arachidonic acid release or calcium mobilization in the CHO cell. The non-cannabinoid receptor-mediated effects of cannabinoid agonists may be related to their hydrophobicity because WIN 55212–2 is considerably less hydrophobic than HU-210 or anandamide.

We were unable to find evidence that the CB_2 receptor couples to either Q-type I_{Ca} or K_{ir} current in AtT-20 cells expressing either high or low levels of CB_2 receptors. AtT-20 cells were chosen for the study because several endogenous ion channels can be modulated by CB_1 when it is expressed in these cells. The observation that CB_2 inhibits adenylate cyclase yet does not activate K_{ir} is intriguing because both of these events are believed to be mediated via G_i. This is unlikely to be a consequence of differential $G_{\alpha i}$ expression in AtT-20 and CHO cells because AtT-20 cells express all three forms of $G_{\alpha i}$ (30). Although the requirement for specific βγ subunits in signaling has been demonstrated (31, 32), the lack of the appropriate βγ subunit expression in the AtT-20 cell is unlikely to be the cause of the failure of the CB_2 receptor to couple to K_{ir}. It has recently been demonstrated that the CB_1 receptor couples to both K_{ir} and inhibition of adenylate cyclase in AtT-20 cells (27). It is not clear why the high expression of CB_2 receptor in AtT-20 cells resulted in a loss of ion channel coupling to cholinergic and somatostatin receptors. It is possible that the presence of high levels of CB_2 receptor could disrupt weak receptor-G protein interactions or sequester G proteins found in limited supply.

Acknowledgments

We are indebted to Monika Holmgren-Konig (Laboratory of Cell Biology, National Institute of Mental Health) and Sidney Bounds (Panlabs, Inc.) for their technical assistance. We would like to thank Michael Brownstein, William Devane, Julius Axelrod, and Miles Herkenham for their invaluable contributions to the manuscript.

References

1. Abood M. E., and B. R. Martin. Neurobiology of marijuana abuse. *Trends Pharmacol. Sci.* **13**:201–206 (1992).
2. Martin B. R., Welch S. P., and M. Abood. Progress toward understanding the cannabinoid receptor and its second messenger systems. *Adv. Pharmacol.* **25**:341–397 (1994).
3. Matsuda, L. A., S. J. Lolait, M. Brownstein, A. Young, and T. I. Bonner. Structure of a cannabinoid receptor and functional expression of the cloned cDNA. *Nature (Lond.)* **346**:561–564 (1990).
4. Munro, S., K. L. Thomas, and M. Abu-Shaar. Molecular characterization of a peripheral receptor for cannabinoids. *Nature (Lond.)* **365**:61–65 (1993).
5. Matsuda, L. A., T. I. Bonner, and S. J. Lolait. Localization of cannabinoid receptor mRNA in rat brain. *J. Comp. Neurol.* **327**:535–550 (1993).
6. Herkenham, M., A. B. Lynn, M. R. Johnson, L. S. Melvin, B. R. de Costa, and K. C. Rice. Characterization and localization of cannabinoid receptors in rat brain: a quantitative *in vitro* autoradiographic study. *J Neurosci.* **11**:563–583 (1991).
7. Mailleux, P., M. Parmentier, and J-J. Vanderhaeghen. Distribution of cannabinoid receptor messenger RNA in the human brain: an *in situ* hybridization histochemistry with oligonucleotides. *Neurosci. Lett.* **143**: 200–204 (1992).
8. Gerard, C. M., C. Mollereau, G. Vassart, and M. Parmentier. Molecular cloning of a human cannabinoid receptor which is also expressed in testis. *Biochem. J.* **279**:129–134 (1991).
9. Devane, W. A., F. A. Dysarz, M. R. Johnson, L. S. Melvin, and A. C. Howlett. Determination and characterization of a cannabinoid receptor in rat brain. *Mol. Pharmacol.* **36**:605–613 (1988).
10. Howlett, A. C., M. R. Johnson, L. S. Melvin, and G. M. Mine. Nonclassical cannabinoid analgetics inhibit adenylate cyclase: development of a cannabinoid receptor model. *Mol. Pharmacol.* **33**:297–302 (1988).
11. Mackie, K., and B. Hille. Cannabinoids inhibit N-type calcium channels in neuroblastoma-glioma cells. *Proc. Natl. Acad. Sci. USA* **89**:3825–3829 (1992).
12. Caufield, M. P., and D. A. Brown. Cannabinoid receptor agonists inhibit Ca^{++} current in NG108–15 neuroblastoma cells via a pertussis toxin-sensitive mechanism. *Br. J. Pharmacol.* **106**:231–232 (1992).
13. Burstein S. Eicosanoids as mediators of cannabinoid action, in *Marijuana/Cannabinoids* (L. Murphy and A. Bartke, eds.). CRC Press, Boca Raton, FL, 73–91 (1992).
14. Reichman M., W. Nen, and L. E. Hokin. Δ9-Tetrahydrocannabinol inhibits arachidonic acid acylation of phospholipids and triacylglycerols in guinea pig cerebral cortex slices. *Mol. Pharmacol.* **40**:547–555 (1991).
15. Felder, C. C., J. S. Veluz, H. L. Williams, E. M. Briley, and L. A. Matsuda. Cannabinoid agonists stimulate both receptor- and non-receptor-mediated signal transduction pathways in cells transfected with and expressing cannabinoid receptor clones. *Mol. Pharmacol.* **42**:838–845 (1992).
16. Devane, W. A., L. Hanus, A. Breuer, R. G. Pertwee, L. A. Stevenson, G. Griffin, D. Gibson, A. Mandelbaum, A. Etinger, and R. Mechoulam. Isolation and structure of a brain constituent that binds to the cannabinoid receptor. *Science (Washington D. C.)* **258**:1946–1949 (1992).
17. Felder, C. C. E. M. Briley, J. Axelrod, J. T. Simpson, K. Mackie, and W. A.

Devane. Anandamide, an endogenous cannabimimetic eicosanoid, binds to the cloned human cannabinoid receptor and stimulates receptor-mediated signal transduction. *Proc. Natl. Acad. Sci. USA* **90:**7656–7660 (1993).
18. Felder, C. C., P. Dieter, J. Kinsella, T. Katsuiko, R. Y. Kanterman, and J. Axelrod. A transfected m5 muscarinic acetylcholine receptor stimulates phospholipase A2 by inducing both calcium influx and activation of protein kinase C. *J. Pharmacol. Exp. Ther.* **255:**1140–1147 (1990).
19. Deutsch D. G., and S. A. Chin. Enzymatic synthesis and degradation of anandamide, a cannabinoid receptor agonist. *Biochem. Pharmacol.* **46:** 791–796 (1993).
20. Childers S. R., Sexton T., and M. B. Roy. Effects of anandamide on cannabinoid receptors in rat brain membranes. *Biochem. Pharmacol.* **47:** 711–715 (1994).
21. Holbrook, P. G., L. K. Pannell, Y. Murata, and J. W. Daly. Molecular species analysis of a product of phospholipase D activation: phosphatidylethanol is formed from phosphatidylcholine in phorbol ester- and bradykinin-stimulated PC12 cells. *J. Biol. Chem.* **267:**16834–16840 (1992).
22. Hamill, O. P., A. Marty, E. Neher, B. Sakmann, and F. J. Sigworth. Improved patch-clamp techniques for high resolution current recording from cell and cell-free membrane patches. *Pflugers Arch.* **391:**85–100 (1981).
23. Johnson, M. R., and Melvin, L. S. The discovery of nonclassical cannabinoid analgetics, in *Cannabinoids as Therapeutic Agents* (R. Mechoulam, ed.). CRC Press, Boca Raton, FL, 121–145 (1986).
24. Devane W. A., Dysarz F. A., Johnson M. R., Melvin L. S., and A. C. Howlett. Determination and characterization of a cannabinoid receptor in rat brain. *Mol. Pharmacol.* **34:**605–613 (1988).
25. Rinaldi-Carmona, M., F. Barth, M. Heaulme, D. Shire, B. Calandra, C. Congy, S. Martinez, J. Maruani, G. Neliat, D. Caput, P. Ferrara, P. Soubrie, J. C. Breliere, and G. L. Fur. SR141716A, a potent and selective antagonist of the brain cannabinoid receptor. *FEBS Lett.* **350:**240–244 (1994).
26. Pinto J. C., F. Potie, K. C. Rice, D. Boring, M. R. Johnson, D. M. Evans, G. H. Wilken, C. H. Cantrell, and A. C. Howlett. Cannabinoid receptor binding and agonist activity of amides and esters of arachidonic acid. *Mol. Pharmacol.* **46:**516–522 (1994).
27. Mackie, K., Y. Lai, R. Westenbroek, and R. Mitchell. Cannabinoids activate an inwardly-rectifying potassium conductance and inhibit Q-type voltage-dependent calcium currents in AtT-20 cells transfected with brain cannabinoid receptor. *J. Neurosci.*, in press.
28. Hanus, L., A. Gopher, S. Almog, and R. Mechoulam. Two new unsaturated fatty acid ethanolamides in brain that bind to the cannabinoid receptor. *J. Med. Chem.* **36:**3032–3034 (1993).
29. Mead, J. F., and W. H. Slaton Jr. Metabolism of essential fatty acids. III. Isolation of 5,8,11-eicosatrienoic acid from fat-deficient rats. *J. Biol. Chem.* **219:**705–709 (1956).
30. Wilson, B. S. M. Komuro, and M. G. Farquhar. Cellular variations in heterotrimer G protein localization and expression in rat pituitary. *Endocrinology* **134:**233–244 (1994).
31. Kleuss, C., H., Scherubl, J. Hescheler, G. Schultz, and B. Wittig. Different β-subunits determine G protein interaction with transmembrane receptors. *Nature (Lond.)* **358:**424–426 (1992).
32. Kleuss, C., H., Scherubl, G. Schultz, and B. Wittig. Selectivity in signal transduction determined by γ subunits of heterotrimeric G proteins. *Science (Washington D. C.)* **259:**832–834 (1993).

Send reprint requests to: Dr. Christian Felder, Laboratory of Cell Biology, Building 36, Room 3A-15, National Institute of Mental Health, 36 Convent Drive MSC 4090, Bethesda, MD 20892-4090.